On neutral particle gravity with nonassociative braids

M. D. Sheppeard

School of Chemical and Physical Sciences
University of Victoria Wellington, New Zealand

Some years ago, Bilson-Thompson [1] characterised the fundamental leptons and quarks using simple three strand ribbon diagrams. These diagrams are interpreted in an abstract categorical language, which underlies an information theoretic quantum gravity. More recently, Graham Dungworth [2] has discussed the astrophysical consequences of this non local quantum gravity, under a symmetry restoring extension of the braid set that doubles the matter sector to include mirror matter. The resulting low energy particle set is reinterpreted in the categorical framework for localization, which considers neutral particle oscillations to be responsible for gravity. A few quantitative observational consequences, such as CPT violation in the neutrino sector, are discussed.

Contents

I.   INTRODUCTION

In demanding emergent classical geometries in a theory of quantum gravity, one must presumably also demand emergent gauge symmetries. Quantum mechanics suggests looking for non localized operations associated to matter states, including mass generation. The notion of spacetime separation should be derived from that of quantum gravitational state. In this light Mach's anti-atomism resurfaces, since one cannot separate spacetime from the matter that defines it. In the context of General Relativity, this issue was first investigated in detail by Roger Penrose, who developed tensor network diagrams [3] and twistors [4].

Here we introduce a modern kind of tensor network, based on braid diagrams for higher dimensional categories. The ambient space of the braids may be viewed as essentially two dimensional, because knots may always be embedded in branched surfaces, a useful trick in dynamical systems theory. Such surfaces are made of glued ribbons, and ribbons themselves may sometimes be defined by their two bounding edge strands. And so, as originally noted by Peano, all higher dimensional spaces may be built from one dimensional ones.

In the last section, we will briefly cover a range of physical consequences of this approach. Although very distinct from popular models for new physics, the ideas discussed here are closely related to the quantum gravity research of Louise Riofrio [5], Matti Pitkanen [6], Carl Brannen [7][8], Graham Dungworth [2], Michael Rios [9], Roger Penrose [4][10] and others. The connection to higher cohomology for twistor theory is not discussed, since the paper should be accessible to a wide audience.

The low energy particle spectrum was given as braid diagrams by Bilson-Thompson [1], without the generation quantum number. Since then, Carl Brannen has shown that generation may be viewed as a tripling of spin [7] in an analysis of noncommutative paths. Category theory will allow us to discuss noncommutative and nonassociative paths in a language that naturally uses braid diagrams. The rest mass quantum numbers may then be analysed, using the full achiral braid set discussed by Dungworth [2].

This full braid set encompasses both the Standard Model spectrum, minus the Higgs boson, and a mirror version of this spectrum. The special role of the neutrino diagrams, along with their observed mixing behaviour, strongly suggests that neutral particle oscillations are responsible for gravity [2]. The simplicity of the exact tribimaximal mixing matrix for neutrinos [11][12] is then a symptom of a simple non local mechanism for gravity.

It is in the nature of mass to be persistent in its existence, in the observer's laboratory. Notions

of time will be considered prior to spacetime, but not in a continuum sense. Rest mass is what it is measured to be: the inertial resistance of a body to changes in motion in an observer's frame of reference. Energy conservation is paramount, but must be considered via underlying concepts in a background independent way. It begins with the discrete time steps associated to measurement events, in the form of CPT symmetries.

The following section outlines the physical framework under which we consider the Bilson-Thompson braid set [1]. Section III discusses the neutral particle diagrams as quantum gravitational operators, and extends this framework to include other quantum numbers. In the final section IV we look at a few remarkable quantitative consequences of this point of view.

II. NEUTRAL PARTICLE GRAVITY

In his *Opticks*, Newton introduces an aether and considers the particle nature of light. His objection to the wave hypothesis of the time was its premise of an inert stage in which waves could propagate. In contrast, the aether was itself a collection of the finest particles, with a tendency to disperse just like a dark energy fluid in the standard cosmology. Light was refracted through its interactions with both matter and the aether. Empty space did not exist.

In a truly quantum universe, where measurement events obtain an ontological status that wave functions cannot, one would like to consider Newton's action at a distance as a statement about separated bodies that does not depend on a fixed background. Consider the first law: objects tend to remain in a state of uniform motion. The two distinct objects being dropped from a leaning tower, by Galileo, begin at rest with respect to each other. Their mutual gravitational attraction is small and directed transversally with respect to the ground below. According to the literal law, there is no reason for these two objects to develop a vertical separation, whether or not the Earth is present. The Earth does not reach out to the locality of the falling masses to affect their relative positions.

How do we measure differences in inertia? In a modern laboratory, the mass spectrometer uses a magnetic field to separate a fixed velocity beam of charged electrons, muons and tau particles. The inertia of the heavier particles gives their trajectories a larger radius. The masses are thus measured by the local rods and clocks of the laboratory, via a circular motion. Similarly, on a pivot weighing scale the heavier side pulls the lighter weight upward in a circular arc about the pivot point. The lighter the mass, the easier its motion is bent.

In these examples, the massive bodies are clearly classical and separated, and the simple notion

of Newton's force may be applied to their dynamics. Newton considered also the spinning bucket. Imagine an ideal liquid in a perfect bucket, so that when the bucket is at rest relative to the human observer, the medium of fluid particles defines a flat surface inside the bucket. When the bucket spins, the surface appears to be curved. The observer does not see the individual particles of the fluid, or the motion of the perfect bucket, but rather one of two static states: a flat surface or a curved surface. Only under the hypothesis of particles do these static observations correspond to rest and circular motion respectively.

As a continuum theory, General Relativity prefers to consider smooth fluids over quantized masses. However, the world is quantum and we should follow Newton in hypothesizing a particle nature for relativistic fluids. Certain new phases of matter, such as the quark gluon plasma, do indeed behave as ideal fluids. Such fluids are often described by classical black hole solutions, through the so called AdS/CFT correspondence. However, this framework assumes a great deal of continuum structure, and insists on giving quantum waves an ontological status that they have not earned.

But if we wish to discuss discrete bodies in our observable universe, is not some a priori classical geometry forced upon us? Not at all, because bodies are not eternal. Like particles in accelerators, they are born and they expire. The Earth may have a somewhat longer existence, and yet by Mach's principle its mass too depends upon the masses of bodies that no longer exist.

A theory of quantum gravity must explain how continuum structures emerge from the abstract information processing of true measurement events. In 1905, the theory of Special Relativity may have banished the materialist ether of waves, but General Relativity then reintroduces a background, in describing the geometry of spacetime concretely in terms of Riemannian geometry. In a quantum theory, General Relativity should eventually be recovered from an entirely different context.

In all of this, the concept of rest mass is a property of discrete bodies, taking certain values from a discrete set. We therefore begin by considering rest mass, and indeed any energy level of any kind, to be a quantum number. These quantum numbers should be defined through the action of simple operators, but these operators need not obey the axioms of ordinary quantum mechanics.

Measurement events are such that there exists a time step, from *before* the event to *after*. Such a causal link will be denoted by an arrow $\rightarrow$ but we do not impose a measure on the time, or associate it directly with a physical continuum. In fact, we do not even assume that these measurement time steps are all governed by the same clocks, since observers will carry their own laboratory clocks around with them.

In this categorical approach, measurement is paramount. We determine our cosmological epoch through the observation of the cosmic microwave background radiation, at a temperature of 2.73 K. Graham Dungworth [2] has recently pointed out that this temperature agrees precisely with the predicted (electron) antineutrino mass of 0.00117 eV [8][13], via Wien's law for black body radiation. Our background of photons is therefore in thermal equilibrium with the antineutrino that commonly partakes in the weak interaction with ordinary matter. If the photons are envisaged as coming from some cosmological horizon, then so are all other forms of matter. A quantum world is *all* Hawking radiation, and the cosmological constant is vanquished in favour of a new anti-realist vacuum fluid aether, modeled observationally by Riofrio's varying speed of light critical density picture, which recovers Kepler's law for orbital motion with respect to a cosmic time measure.

Already there are two times to consider in the definition of operators: local laboratory clock ticks and an observer's cosmological clock. These times are *observer dependent*, and we do not assume that a neutrino who rushes through our laboratory concurs with our measurement of times. Mass operators will be defined as information transfers with respect to observer clocks. So like in quantum mechanics, there is given a notion of event time with respect to which processes happen. Also as in quantum mechanics, non locality and entanglement are features. However, mass generation must break the rules of quantum mechanics.

Measurement algebras become more important than the concept of state or wave function. The initial aim is to understand the origins of the Koide mass matrices [8], from a two time perspective. Arrows as processes will define categorical diagrams for mass operators.

A. A Categorical Framework

An abstract category generalises the notion of set elements to arrow like objects. Whereas a set has only one level of axiomatic structure, namely the *element*, a D dimensional category has $D+1$ levels of structure, namely points, line arrows between points, directed areas between arrows, and so on. This language is sufficiently foundational that it will provide links with many related aspects of mathematical physics.

Collections of oriented line segments may form pieces of knot diagrams in three dimensional space. We will be interested in diagrams on a page, but with marked over or under crossings where they occur. These are to be viewed as describing a generalisation of Venn diagrams for set theory Boolean logic. With a Venn diagram, a closed loop defines a disjoint interior and exterior, denoting a set S and its complement NOT S, with respect to some universal set. By allowing braid

diagrams, we relax the Boolean logic of sets.

A mass measurement is a three outcome experiment, which we would like to describe using a ternary logic of outcome possibilities. Braid diagrams in the page will be restricted to three strand pictures, since this case will nicely cover the low energy particle spectrum, much as two strands are used to describe a basic entangled state for two qubits [14]. However, instead of Hilbert spaces constructed with ordinary † dualities, the dualities that appear in braid diagrams are naturally associated to the discrete particle symmetries P and T. Non Hermitian types of quantum mechanics are well studied in this context. Nonassociativity adds the discrete C symmetry.

Observe that a general braid diagram in a plane defines two directions: horizontal and vertical. These directions will represent two distinct observer time measurements. Vertical time, arbitrarily directed down the page, will be a laboratory passage of time, which occurs with every measurement event. Reversal of this time direction mimics time reversibility in ordinary quantum physics, only now braid diagrams will no longer be time symmetric. The horizontal coordinate brings in a cosmological time factor, which in a sense is fixed here by the three strands of the low energy spectrum.

A reflection across the vertical axis turns left handed particles into their right handed mirror partners, of like charge. Horizontal reflections similarly swap chirality. Vertical braid compositions are used to describe pair annihilation. The full picture is achiral, since all chiral braids have mirror partners.

Once the low energy particle spectrum is described by the Bilson-Thompson braids [1], we would like to assign operators to the braids. A braid from 3 points to 3 points, down the page, will have strands labeled by letters X, Y or Z. These are qutrit quantum numbers. The ordering of strands defines a word in the three letters. Nonassociativity, as in $X(YY)$ for a quark state, gives a doubling of length 3 words, from 27 to 54.

We would also like to associate matrix operators to the braid algebra. For a three strand braid on the word ABC, a possible matrix array has the form

$$\begin{pmatrix} AA & AB & AC \\ BA & BB & BC \\ CA & CB & CC \end{pmatrix} \tag{1}$$

When A, B and C are commutative numbers, this matrix has zero minors. Later on we will associate entropy measures to combinations of matrix minors, and such a commutative matrix has zero entropy. In order to understand these operators in a type of path integral context, we first consider the enumeration of finite length noncommutative and nonassociative paths [7].

B. Noncommutative and Nonassociative Paths

For n variables the commutative monomials of degree d may be listed on the nodes of a divided triangular simplex, as indicated in figure 2. These simplices are a reduction of noncommutative paths on a cubic lattice. For example, figure 1 shows how length 2 paths are projected onto a diagonal line of length $d = 2$. Length 1 paths for n variables result in a standard simplex of dimension $n - 1$, but this $d = 1$ column may be projected onto polygons in the plane.

FIG. 1: Commutative quotient of length 2 noncommutative path space

As in figure 2, the case $(n, d) = (3, 3)$ recovers the Pythagorean tetractys from the 27 trit paths of length 3 on a cube. The ten vertices of the tetractys partition the 27 paths according to the number of neighbouring vertices, when an outer edge neighbour is given a half weight. Thus a corner corresponds to a single path, an outer midpoint three paths, and the central vertex represents six paths. This number $27 = 3^3$ notoriously appears as a coefficient in the discriminant of a cubic polynomial [17].
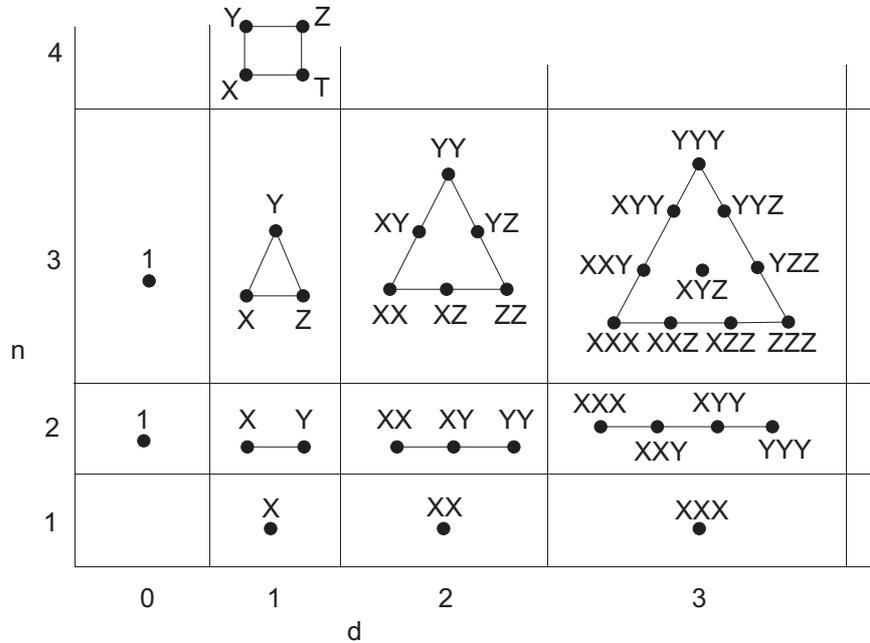

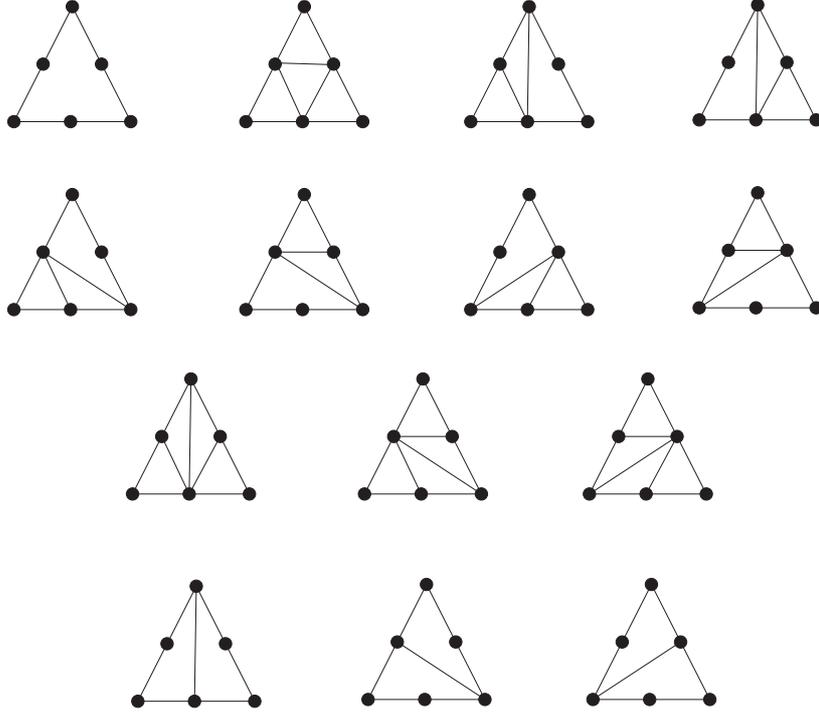FIG. 2: Monomial table in variable number and path length

FIG. 3: Vertices of the three dimensional associahedron

In the Jordan algebra setting discussed in [9], which is associated to the black hole entropy entanglement correspondence in M Theory, the complex dimension 27 appears in a 2×2 Freudenthal triple system, which recovers the 56 dimensions associated to an E_6 symmetry. We are also interested in 57 dimensional ternary analogues of this basic duality bioctonion algebra, given by the two dimension structures

$$\begin{pmatrix} 1 & 27 \\ 27 & 1 \end{pmatrix} \quad \mapsto \quad \begin{pmatrix} 1 & 9 & 9 \\ 9 & 1 & 9 \\ 9 & 9 & 1 \end{pmatrix} \quad \text{or} \quad \begin{pmatrix} 3 & 8 & 8 \\ 8 & 3 & 8 \\ 8 & 8 & 3 \end{pmatrix} \tag{2}$$

which we observe can be read off the tetractys and its neighbours to the left (two qutrits) and downwards (three qubits). The top right sections of these matrices are given by right concatenation of a letter onto a length two path, whereas the lower left sections come from left concatenation. The diagonal of ones is the embedding of ordinary geometric duality, between points and lines, to the classical duality on points, lines and faces. The diagonal 3 elements belong wholly to ternary geometry.

Let us normalise the area of a minimal piece inside any triangulated simplex to 1. Zero area triangles are also permitted along a simplex edge. For the tetractys the possible triangle areas are $0, 1, 2, 3, 4, 6$ and 9. That is, volumes take values $V \in \{2^{i_2} 3^{i_3} \cdots d^{i_d}\}$ for $i_k \leq n - 1$. The 14

possible triangulations for $(n, d) = (3, 2)$ are given in figure 3. Since this simplex is essentially a hexagon, these are the vertices of the associahedron polytope in dimension 3 [17]. The 21 edges of this associahedron are usually labeled by hexagons which are only partially triangulated, which is to say that one internal chord is missing. In figure 3 each triangle has three chords, since an isolated edge of three vertices counts as a chord, so an associahedron edge exists if there is only one chord flip between diagrams. Each chord can always be flipped across the square that it defines, showing that the associahedron graph is trivalent.

To each set $S(n, d)$ of simplex points one may assign a *secondary polytope* [17] that is the convex hull of certain vertices given by allowed triangulations. For the polygons of the column $d = 1$, this gives the associahedron in dimension $n - 3$. For the measured intervals of the row $n = 2$, this polytope is a cube of dimension $d - 1$. For example, the length 3 interval $S(2, 3)$ maps to a square with vertices matching the partitions $(1, 1, 1)$, $(1, 2)$, $(2, 1)$ and (3). Along the row $n = 2$ there is an obvious map $P(2, d)$ taking noncommutative paths for $S(2, d)$ to the partitions of the cube polytope for $S(2, d + 1)$, as in figure 4. Moving up columns, there is an embedding $v(n, d)$ of a simplex $S(n, d)$ into the simplex $S(n + 1, d)$, and moving along rows there is an embedding $h(n, d)$ into one corner of the larger simplex.
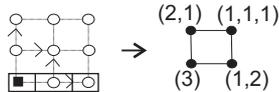

FIG. 4: Noncommutative paths as partitions on a cubic polytope

Simplices may be coordinatised [17] according to the monomial labels. For example, the monomial $X^3 Y^2 Z$ in $S(3, 6)$ is given the coordinate vector $(3, 2, 1)$ of entry sum $d = 6$ in $\mathbb{R}^3$. The homogeneity of monomial degree means that all points in the higher dimensional $S(n, d)$ lie in the hyperplane

$$x_1 + x_2 + \cdots + x_n = d \tag{3}$$

for vector coordinates x_i. This fixes a volume normalisation factor for the simplex. Integral coordinates will be abbreviated so that $(3, 2, 1)$ becomes 321.

Permutations on three letters, such as 321 or 231, may be represented by three strand string diagrams between three points (labeled 1, 2 and 3), as in the right hand side of figure 9, ignoring the knot crossings. Thus the set on which the permutation acts becomes an object in a category whose arrows are string diagrams.

The physical emphasis on measurement operations, rather than states, is thus responsible for the introduction of a new level of categorical structure. In what follows, we do not assume that the three point object sets belong to an ordinary category of sets. In fact, the category of sets is *not* a braided category. One may view the n point sets as arithmetic sets, which are linear spaces over the field with one element, since they are closely associated to a quantum mechanical representation of finite field arithmetic [18]. As discussed below and elsewhere [19], the braiding is a required component of mass generation through the introduction of time asymmetries.

III.   CATEGORICAL DIAGRAMS FOR GRAVITY

One strong motivation for studying physics with diagrams from category theory is the potential of such methods to provide real world computations without invoking unnecessary and difficult continua. The banishment of the absolute background is seen as an essential element of an emergent classical spacetime in quantum gravity.

A braid or ribbon diagram consists of strands with endpoints in the upper and lower sides of a diagram. These diagrams make sense in a large interesting class of categories, such as representation categories for Hopf algebras. Using ribbon strands, we find many connections with deep mathematics, such as Grothendieck's children's drawings.

As discussed by Shum [20], a ribbon segment may be described by two bounding strands, placed near to one another. In general, it is useful to group strands according to the bracketing of the tensor product of objects that is being represented by the full strand set. That is, once we insist on distinguishing ribbon edge pairs from separated strands, we might as well look at diagrams with mixtures of ribbon and strand elements.

In [1] the fundamental fermions of the Standard Model are listed in terms of three braided ribbon segments. A ribbon segment is represented by two nearby strands, for a total of six single strands in each diagram. However, since the ribbons of neutral fermions remain untwisted, in this case the two ribbon edges may be replaced by a single strand, as in the right hand side of figure 9. Thus all possible neutral particle braids are given by a three strand diagram, including all possible reflections both vertically and horizontally in the page.

A reflection across the vertical axis performs both a left right mirror and a matter to antimatter conjugation, while the horizontal axis reflection is a left right mirror only. The four possible braids of the type shown in figure 9 then correspond to the four chiral neutrinos and antineutrinos, ν_L, ν_R, $\overline{\nu}_R$ and $\overline{\nu}_L$.

The chiral charged leptons and quarks are described by putting twisted ribbon charges in place of these neutral strands. The paths for the quarks and leptons are given by the tetractys diagram:

charged leptons: XXX, YYY, ZZZ

up quarks: XXY, XYX, YXX

down quarks: XYY, YYX, YXY

neutrinos: XYZ and permutations.

The path count is doubled with the addition of brackets. With this introduction of mass quantum numbers there is a total of 27 chiral fermions for the electroweak sector. All neutrinos and mirror neutrinos are counted. Although these particles may be mapped to boson diagrams via a generalized quantum Fourier transform, there is no Higgs boson. In [1] it was shown that basic interaction rules are obeyed by braid compositions.

The question is: why do these particular diagrams capture the low energy fermion spectrum? Here we will begin to reinterpret the particle braids using trivalent vertices, which are mixtures of single strands and ribbon segments. Unlike the morphisms of the symmetric monoidal categories of quantum mechanical computation [21][14], our arrows will be braided and nonassociative.

A.   Localization

With an aim to understanding the quantum gravitational context of such diagrams, observe that Standard Model localization is viewed as an emergent feature in modern on-shell twistor space techniques for particle scattering [22][23][24][25][19]. Here scattering amplitudes for n particles may be constructed using a recursive procedure that begins with the three particle case. However, physical amplitudes begin at $n = 4$, which appears with the decomposition of a 4-valent graph into two trivalent pieces, as in figure 5. Categorically speaking, the four particle case is associated to an associahedron point, whereas a trivalent node denotes an empty associahedron. In other words, space begins with four things, but it arises from nothingness.
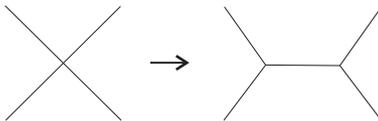

FIG. 5: Localization as factorization

The weak interaction is now viewed as a four particle process, with two neutrinos involved in beta decay. The next section outlines the particle diagram elements that appear natural from a

categorical perspective, and the final section discusses a few physical consequences of this framework.

B. Mixed Strand and Ribbon Diagrams

Braid or ribbon diagrams are neatly oriented in the plane of the page, so that they may be composed via concatenation. In mixed diagrams, ribbons are joined to ribbons and strands to strands. We consider diagrams from three points to three points, where the fixed three point set is associated to the generation mass quantum number as a ternary analogue of dualities associated to two ribbon edges.

An algebraic (or coalgebraic) object in a symmetric monoidal category, where the braid crossings are ignored, is usually represented by a trivalent node. However, the real conundrum of figure 5 is that the tree diagram for the empty three particle associahedron should be represented by a two leg tree, as shown in figure 6, where the signs often stand for particle helicity [23]. For each particle number n there should be a reduction to $n-1$ tree legs, through the selection of a root ribbon leg. Thus a four particle diagram becomes the simplest possible rooted tree with two branches, known as the associahedron point. Such a replacement of nodes by braid crossings is also familiar in the modern renormalisation theory of Kreimer, Broadhurst, Connes and others.
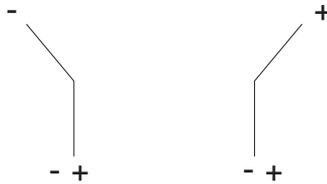

FIG. 6: Three particle rooted trees

The allowed trivalent mixed diagrams are then given in figure 7. Arbitrary networks may be created from these six vertex types. By shrinking ribbons to strands, and ignoring crossings, we recover the unique unlabeled trivalent node of a symmetric monoidal category.
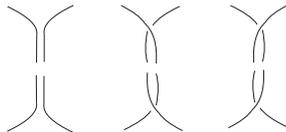

FIG. 7: Six trivalent vertex types

Networks are built from the trivalent vertices, and $n \times n$ matrices may be associated to networks between two sets of n points. This can be generalised to hypermatrices of dimension k for any number of k sets of n points. The fixed point set represents a fixed low dimensional object in the category, and nonassociative braid networks are single arrows of the form $\mathbf{n} \to \mathbf{n}$. For $k > 2$, multiarrows are permitted. Using the allowed vertices of figure 7, the simplest possible arrows are those on two strands between two sets of two points.
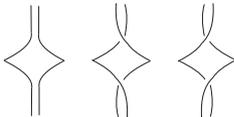

FIG. 8: The three $F \circ F^*$ ribbons

Figure 8 shows the three possible arrows of the form $F \circ F^*$, where F^* is the dual vertex given by a reflection in the horizontal axis, which happens to be the same as F. Such reflections send ordinary matter to opposite chirality matter. These single ribbons represent [1] electric charges of $0, \pm 1/3$, and triplets of such ribbons give the particle spectrum of the Standard Model.

Ternary braid arrows are now constructed from dual pair arrows, G and $G^\dagger$, where the $\dagger$ dual consists of reflections in both the horizontal and vertical axes. This dual sends a particle to its same chirality mirror particle. Identity strands may also be inserted. The insistence on mirror duality is a physical condition that will be associated to a cosmological time asymmetry, whereby the local time reversibility of quantum field theory is maintained by the $*$ dual, while the cosmological time exhibits asymmetry.

Restricting attention to three strands, consider the particle braid on the right hand side of figure 9. This is constructed out of four trivalent diagrams as shown, where ribbon segments join ribbons and strands join strands. The lower pair is the $\dagger$ dual of the upper pair. As a categorical morphism $f : \mathbf{3} \to \mathbf{3}$, this braid takes the form $f = (F \otimes I) \circ (I \otimes F^\dagger)$, with F a four leg diagram with one crossing. The two ribbon segments on the left hand side are introduced as a categorical localization procedure (see figure 5) without which the morphism f would just be given by two 4-valent symmetric crossings. These are the simplest possible dual pair braids on three strands.

Note that the symmetric quantum mechanical reduction to a unique vertex [14], where all ribbons are shrunk and crossings ignored, assumes a fixed time reversibility. The braiding vertices are required to account for the new time asymmetries. An observer's thermodynamic arrow of cosmic time is asymmetric. This will be discussed in the final section.
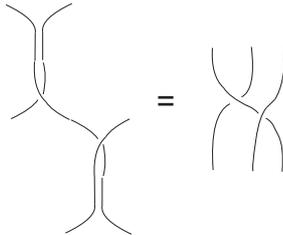
FIG. 9: Composition of 4-valent segment with its dual

We are not only interested in monoidal structure. The remaining asymmetries, which do not allow us to reduce ribbons to strands, will be directly associated with a breaking of monoidal structure in tricategories, where the pentagon law lies on five sides of a cube [19]. A true three dimensional arrow may fill this axiomatic cube for tricategories. The most interesting feature in this dimension is the existence of a *dimension raising* tensor product, where Space is being created.

C.   Extension to General Quantum Numbers

Figure 8 gives the twisted ribbons that represent electric charge [1]. If we allow the single strands of a three strand braid to become any of the three charged ribbons, we obtain all the lepton and quark braid diagrams [1]. Quark color is given by the three possible choices of position for twisted ribbons, and is hence marked by the letters on a braid. Both left and right handed leptons and quarks are obtained in this way.

Once particle generation is recovered as a quantum number [7], these braid diagrams catalogue the low energy Standard Model particle spectrum and a mirrored version of it. A subset, in simplified matrix form, is given in figure 10. As shown in [16], the bosons are obtained from the fermions via a twisted Fourier transform, where the twisting uses the reflections of the braid diagrams. They include a photon, W^+ and W^- bosons, coming from left handed leptons, and then a color triplet of preons for the Z boson, coming from the three right handed leptons. As for the strong interaction, Z boson color appears to be confined at low energy. This confinement is now associated to the hidden right handed sector of mirror leptons. The quark sector also results in boson matrices, but they are not expressible as three strand braids [16].

Observe how the whole neutral particle sector mixes ordinary matter and the mirror form of matter. We will see that neutrinos have different masses to their corresponding antineutrinos. As discussed by Dungworth [2], this means that, unlike the charged particles, the ordinary antineutrino $\overline{\nu}_R$ annihilates with its mirror matter antineutrino $\overline{\nu}_L$. What are usually considered mass states

in neutrino or antineutrino oscillations are in fact mass states for pairs of particles, one living in the mirror matter sector. These mass states are achiral, being composed of a left handed and right handed piece.

This non local process is hypothesised to be responsible for quantum gravity. The primary local rule is one of energy conservation, which is now expressed via perfect CPT symmetry across all mass energy components. That is, when manifest chirality exhibits itself in the weak interaction, it hides a mirror process involving the opposite chirality antineutrino. Charge and parity are really conserved. The two distinct notions of time, one cosmological and one local, may be asymmetric in our ordinary matter sector, but a time symmetry is restored across the mirror. Proponents of cyclic cosmologies [10] or multiverses would probably view this mirror sector as inhabiting another universe, but an observer lives in only one personal universe and our mirror presumably takes us into the dark matter sector.

$$
\begin{array}{cccccc}
e_L^- & e_L^+ & e_R^- & e_R^+ & \nu_L & \bar{\nu}_R
\end{array}
$$

$$
\begin{pmatrix} 0 & \bar\omega & 0 \\ 0 & 0 & \bar\omega \\ \bar\omega & 0 & 0 \end{pmatrix}
\begin{pmatrix} 0 & \omega & 0 \\ 0 & 0 & \omega \\ \omega & 0 & 0 \end{pmatrix}
\begin{pmatrix} 0 & 0 & \bar\omega \\ \bar\omega & 0 & 0 \\ 0 & \bar\omega & 0 \end{pmatrix}
\begin{pmatrix} 0 & 0 & \omega \\ \omega & 0 & 0 \\ 0 & \omega & 0 \end{pmatrix}
\begin{pmatrix} 0 & 1 & 0 \\ 0 & 0 & 1 \\ 1 & 0 & 0 \end{pmatrix}
\begin{pmatrix} 0 & 0 & 1 \\ 1 & 0 & 0 \\ 0 & 1 & 0 \end{pmatrix}
$$

$$
\begin{array}{cccccc}
\bar{u}_L(1) & \bar{u}_L(2) & \bar{u}_L(3) & d_R(1) & d_R(2) & \bar{d}_R(1)
\end{array}
$$

$$
\begin{pmatrix} 0 & \bar\omega & 0 \\ 0 & 0 & \bar\omega \\ 1 & 0 & 0 \end{pmatrix}
\begin{pmatrix} 0 & 1 & 0 \\ 0 & 0 & \bar\omega \\ \bar\omega & 0 & 0 \end{pmatrix}
\begin{pmatrix} 0 & \bar\omega & 0 \\ 0 & 0 & 1 \\ \bar\omega & 0 & 0 \end{pmatrix}
\begin{pmatrix} 0 & 0 & \bar\omega \\ 1 & 0 & 0 \\ 0 & 1 & 0 \end{pmatrix}
\begin{pmatrix} 0 & 0 & 1 \\ \bar\omega & 0 & 0 \\ 0 & 1 & 0 \end{pmatrix}
\begin{pmatrix} 0 & 0 & \omega \\ 1 & 0 & 0 \\ 0 & 1 & 0 \end{pmatrix}
$$

FIG. 10: Quark and lepton braids

IV. OBSERVATIONAL CONSEQUENCES

The braid and ribbon diagrams are now interpreted in this multiple time cosmology, wherein mass generation requires at least one observer measurement time along with a selection of cosmological scale. The horizontal time direction, which appears in † duality, counts information dimension, and a reflection in this direction flips the chirality of a particle. Vertically, the ∗ reflection flips both chirality and matter types, as for the usual local reversible time of quantum fields. The combination † duality fixes chirality, but sends a particle to its mirror sector antiparticle.

In principle, the framework respects the M theoretic dualities associated to the three qubits that are studied in the black hole entropy entanglement correspondence [28]. This includes an S duality that interchanges the largest and smallest physical scales, and is associated to electric charge locally.

An observer must separate disparate scales from the central scale of observation. The number of braid strands is thus viewed as an extensivity constraint for the measurement clocks. Ribbon localization is then a forced extension of four particle vertices into both cosmological and local time. There are no events without time steps, and all fundamental interactions are essentially four, or rather eight, particle ones.

Riofrio [5] describes the whole dark matter sector in terms of black holes, and this is a useful way of visualising our thermodynamic arrow of time, by setting a cosmological clock to zero at a prior cosmological horizon, and infinity at future horizons. Braid strands stretch through local measurement time, and mark a fixed cosmological scale horizontally.

There is quantitative evidence to support this point of view. The next section summarises results on mixing matrices and the Koide mass operators, and then we briefly mention a few of the astrophysical consequences of this framework.

A.   Mixing Matrices and Koide Mass Triplets

As discussed in [15], the exact neutrino tribimaximal mixing matrix [11][12] may be expressed simply in a variety of forms that directly exhibit its lack of CP violation. In particular, a signed set of the nine real entries appears in the Koide eigenvalue [8] triplet

$$\lambda_1 = \sqrt{\frac{1}{3}} + \sqrt{\frac{2}{3}}\cos\delta + \sqrt{0}\sin\delta \tag{4}$$
$$\lambda_2 = \sqrt{\frac{1}{3}} - \sqrt{\frac{1}{6}}\cos\delta - \sqrt{\frac{1}{2}}\sin\delta$$
$$\lambda_3 = \sqrt{\frac{1}{3}} - \sqrt{\frac{1}{6}}\cos\delta + \sqrt{\frac{1}{2}}\sin\delta$$

which for $m_i = \lambda_i^2$ recovers the masses [8] of all leptons: charged leptons at $\delta = 2/9$, neutrinos at $\delta = 2/9 + \pi/12$ and differing mass antineutrinos at $\delta = 2/9 - \pi/12$. The inaccurately known up quark masses are fitted to a Koide triplet with the exact phase $\delta = 2/27$, and with the $\sqrt{2}$ parameter that defines tribimaximal mixing replaced by $r(\delta) = \sqrt{2}\sin(5\pi/6 - 2/9 + \delta)/\sin(\pi/6)$. The blogger Dave Look has pointed out that this r value is defined geometrically by inscribing the charged lepton triangle at radius $\sqrt{2}$ inside the up quark triangle, so that the charged leptons lie on lines between quarks. Related r and δ values may be used to define a down quark mass triplet, although the parameters are difficult to fix with current experimental accuracies. In particular, the values $r = r(2/27)$ and $\delta = 4/27$ approximate the down quark mass triplet.

For leptons $r = \sqrt{2}$, which comes from the neutrino mixing matrix [11][12] as follows. Let θ be

the angle such that $\sin\theta = 1/\sqrt{3}$, using the information normalisation for dimension 3 matrices. Then $\tan\theta = \sqrt{2}^{-1}$. It is this tangent that is used as a basic mixing parameter, as explained in [15].

Thus, although a scale factor μ is selected arbitrarily at present, all fundamental leptons are associated to a few special phases used to define Koide triplets. The parameters of the Standard Model are thus greatly reduced. Now we would like to understand how the Koide matrices

$$\sqrt{M} = \mu \begin{pmatrix} 2 & re^{i\delta} & re^{-i\delta} \\ re^{-i\delta} & 2 & re^{i\delta} \\ re^{i\delta} & re^{-i\delta} & 2 \end{pmatrix} \tag{5}$$

are associated to particle braids. The three strand diagrams $f : \mathbf{3} \to \mathbf{3}$ must be associated to 3×3 matrices, but these are not necessarily viewed as elements of a linear algebra. Recall that the most basic braid matrices had rows and columns indexed by the object set A, B and C, so that the nine entries cover all possible length two noncommutative paths in these letters. In contrast, a Koide matrix uses at least length three paths to define its phases [8].

The Koide matrix is a 1-circulant discrete Fourier series, with basis the three odd permutations on three letters. The two non identity permutations are those underlying the three strand particle braids. An annihilating pair of neutrinos provides one such pair. Without an identity component, the eigenvalue sum is zero, so the identity is essential in characterising observable triplets.

We may imagine that positive rest mass is extracted from a zero mass energy operator Z, with three zero eigenvalues split by the complex decomposition $Z = \sqrt{M} + i\sqrt{M}$. The Koide matrix $\sqrt{M}$ is a Fourier transform of a diagonal matrix, and has been used by Brannen to fit both the lepton and many hadron masses [8]. It has only one off diagonal phase. In particular, note again that the neutrino and antineutrino mass predictions [7][13] follow from the phase choices

$$\nu : \quad \delta = \frac{2}{9} + \frac{\pi}{12} \qquad\qquad \bar{\nu} : \quad \delta = \frac{2}{9} - \frac{\pi}{12}$$

where Brannen's [7] Berry phase of $\pi/12$ appears naturally in the noncommutative path integral representation of generation number. Here it represents the 24 information dimensions spanned by standard particles [16], and the $\pi/12$ sign change interchanges left handed particles with right handed ones. Since total phase conjugation gives us some freedom in sign choices, the pair $\pm\pi/12$ may be associated to annihilating particle pairs. In fact, a matrix representation of braid generators automatically gives us a matrix representation of the root, $A^{24} = 1$.

The phase $+2/9$ usually appears in all ordinary matter Koide triplet fits, but we are free to use it here to label left handed particles, with right handed particles taking the negative phase. This

associates the universal 2/9 with the horizontal cosmological time. The origin of the 2/9 remains a little unclear, but here it will represent the fraction 6/27 of noncommutative paths that involve all three directions: X, Y and Z. If the 2 in the numerator is absorbed into a missing 2π, this is reduced to 3/27, which precisely accounts for the 1-circulant paths underlying the mass operators. These are the paths used to derive the other component of the phase [7].

The missing factor of 2π in the phase 2/9 could then be due to a mismatch between a local orbital Keplerian time and Riofrio's radial cosmic time, which represents an evolving universal mass from a zero mass cosmological horizon. That is, Riofrio's version of Kepler's law employs a radial cosmic time parameter that differs by a factor of 2π from the usual Keplerian time. The like sign nature of the double phases in [8] is then explained by the standard matter type of hadrons.

Phases are typically computed as areas enclosed by paths, and areas can be either positive or negative, as in modern symplectic geometry. The $\pi/12$ phases are thought of as triangular pieces of a marked surface whose area sum is 2π, like the circumference of an orbit [7]. In figure 11, a $\pi/12$ segment is a one third section of a $\pi/4$ triangle. This graph uses an area normalisation of π for the non zero triangles of the path simplex, for a total of 2π both inside and outside this area. To obtain the more common word representation, we reduce the X, Y and Z variables using Pauli matrix rules. But using the given tetractys labels of figure 11, the 2/9 is the path count at the central vertex. In other words, to obtain the 2/9 phase we imagine a dual surface with phase sum 1, representing the length three path fraction 27/27.
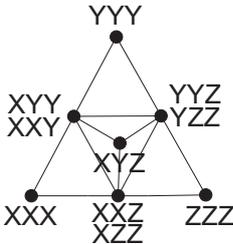
FIG. 11: Berry phase diagram for three qutrits

The dual graph to the tetractys is the honeycomb network of figure 12. This is the simplest trivalent network with three leg triplets that contains an internal area, and we observe that this hexagon area comes from the 2/9 vertex. The other pieces of the plane are similarly labeled by path fractions. The dual graph of the reduced tetractys is a six leg diagram with a triangle at the central trivalent node.

Now observe that the full lepton set of three Koide eigenvalue triplets may be expressed directly
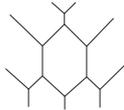
FIG. 12: Dual tetractys as trivalent network

in terms of the nine entries of the tribimaximal neutrino mixing matrix, via multiplication by a second phased matrix, namely

$$
\frac{1}{3}
\begin{pmatrix}
1 & \sqrt{2} & 0 \\
1 & -\sqrt{2}^{-1} & -\sqrt{3/2} \\
1 & -\sqrt{2}^{-1} & +\sqrt{3/2}
\end{pmatrix}
\begin{pmatrix}
1 & 1 & 1 \\
\cos(2/9) & \cos(2/9 + \pi/12) & \cos(2/9 - \pi/12) \\
\sin(2/9) & \sin(2/9 + \pi/12) & \sin(2/9 - \pi/12)
\end{pmatrix}
\tag{6}
$$

where the left hand factor is the tribimaximal matrix, which may be expressed in a phase form similar to the right hand factor, but with the 2/9 replaced by zero and the $\pi/12$ replaced by the cubed root of unity. By altering the mixing matrix and the phases of the right hand factor, any Koide triplet may be expressed this way.

The CPT violation recently observed by MINOS [29] agrees quantitatively with the Δm^2 values given by the neutrino and antineutrino Koide triplets [13][15]. As noted below, the more precisely known value of the CMB temperature may be used to better constrain the Koide fits to MINOS results, and tighten other predictions. The difference in neutrino and antineutrino masses relies on the existence of one negative eigenvalue, for the electron neutrino, which has the lightest of all masses at 0.00038 eV. This does not occur for the charged leptons, whose mass equivalence is exact under the phase choices given here, even when the 2/9 is offset by a small correction of π/n for large n. This reflects the symmetry of charged lepton braid words, of type $X(XX)$.

In an ongoing study of particle mixing, we suppose a tight relation between particle oscillations and potential mass differences. A matter antimatter mass difference is also observed for neutrons, although the statistical significance of this result is currently poor. Like the neutrinos and antineutrinos, the neutrons could oscillate with their mirror matter without violating current experimental bounds [30].

The ν and $\overline{\nu}$ triplets are thus distinguished by a sign match or mismatch, rather than an absolute choice of overall sign. This is in line with Dungworth's suggestion [2] that the ν and $\overline{\nu}$ triplets be split into annihilating equal mass pairs, giving the doubling of neutral braid states. This conveniently associates the four possible neutrino phase choices precisely with the four neutrino braids. The phase $+2/9$ is for the $(\overline{\nu}_L, \nu_L)$ pair, while $-2/9$ selects the right handed neutral pair.

An alternative phase choice is shown in figure 13, where the $+2/9$ phase corresponds to the ordinary matter sector.

$$+\frac{2}{9}+\frac{\pi}{12} \qquad -\frac{2}{9}+\frac{\pi}{12} \qquad +\frac{2}{9}-\frac{\pi}{12} \qquad -\frac{2}{9}-\frac{\pi}{12}$$

$$\nu_L \qquad\qquad \bar{\nu}_L \qquad\qquad \bar{\nu}_R \qquad\qquad \nu_R$$

FIG. 13: Four neutral braids with Koide phases

Observe that the two antineutrino phases involve a sign mismatch, but either choice results in the same mass triplet. Similarly, the ν_L matter particle annihilates with its mirror ν_R. This annihilation to a photon is given by vertical braid composition, resulting in the identity photon braid. In this scheme, the β^- decay

$$n \;\;\rightarrow\;\; p^+ \;\;+\;\; e^- \;\;+\;\; \bar{\nu}_R$$

is a four particle process that secretly borrows the $\bar{\nu}_L$ mirror particle (not a lepton) from the cosmic vacuum. We imagine a whole mirror beta decay process, which could well be real, so that parity, charge and lepton numbers are all conserved. The mirror process suggests a mirror neutron, which would oscillate with ordinary neutrons. This in turn suggests a whole hierarchy of neutral particles, that oscillate with the mirror sector. An initial description of the neutron might use the nine strand diagram constructed from the three component quark braids.

Observe that the $\pi/12$ phase appears only for mixed matter annihilating pairs, such as (ν_L, ν_R). If the charged lepton phase has an additional π/n component, n must be large, in line with the idea that charge carries considerable information. The $*$ duality, used in defining charge ribbons, flips the sign of the $\pi/12$ phase, but under $\dagger$ duality this chiral phase is invariant. The associated 24 dimensional space may be thought of as a minimal holographic information space, spanned by particle quantum number sets.

Michael Rios has pointed out that the four neutrino braids correspond to very simple expressions in terms of generators for the modular group, which is obtained as a quotient of the braid group

on three strands. Letting the modular group generators be

$$A = \begin{pmatrix} 1 & 1 \\ 0 & 1 \end{pmatrix} \quad B = \begin{pmatrix} 1 & 0 \\ -1 & 1 \end{pmatrix} \tag{7}$$

the correspondence may be given by

$$\nu_L = B^{-1}A \quad \nu_R = A^{-1}B \quad \bar{\nu}_L = BA^{-1} \quad \bar{\nu}_R = AB^{-1}$$

Considering a separate copy of a braid for each generation, we imagine three copies of the modular group, namely the three qubit entanglement group of M theory [28]. These S, T and U duality groups are now seen to describe the tripling of spin that was used by Brannen [7] to derive generation operators.

B.   Initial Astrophysical Implications

The rest mass predictions for the neutrino sector use a scale of $\mu = 0.01\sqrt{eV}$, and include an (electron) antineutrino mass of 0.00117 eV [13]. In the full braid spectrum, this mass energy is shared between the antineutrino $\bar{\nu}_R$ and its mirror dark neutrino, the $\bar{\nu}_L$, which annihilate to photons. Graham Dungworth [2] has pointed out that this mass energy corresponds precisely, under Wien's law for black body radiation, to a temperature of 2.73 K, which we recognise as the observed temperature of the cosmic microwave background radiation. The next lightest neutrino mass corresponds to the CMB appearance temperature that we observe at a redshift of $z = 6.6$ (to appear). We now expect interesting features in redshift surveys for such values of z. Similarly for the special redshifts associated to the heavier neutrinos.

The antineutrino thus sets the human observer's thermodynamic cosmic clock, and destroys the standard Big Bang picture of classical local evolution from a singular beginning. The image of an expanding universe survives, but we are now forced to acknowledge the non local nature of quantum causality and its ability to prohibit the ontological reality of singularities through the presence of horizons.

Riofrio's [31] varying c picture, which hinges on the law $GM = Tc^3$ for a universal mass M, may alternatively be interpreted as an evolution of mass with cosmic time T. This directly associates zero mass states with a cosmological horizon, as in Penrose's classical thermodynamic cosmology [10]. The varying c version of Riofrio's law neatly accounts for the anomalous redshifts in type IA supernovae, the horizon problem (which disappears entirely with the $c = \infty$ limit), the Pioneer

anomaly, lunar laser ranging anomalies, the zero angular correlation of the CMB at large angles, and so on.

Dungworth also discusses other astrophysical consequences of both the light neutrino masses and the mirror dark matter that results from the opposite chirality braids. Although usually discussed in the context of the old Standard Model, mirror matter has a long history and is studied by many as a dark matter candidate. For instance, R. Foot [30] has considered many observations, such as the positive DAMA modulation results. Here however, the only mirror matter that is forced upon us are the neutrinos and antineutrinos.

Further consequences of neutrino gravity will be considered in other work.

C.   Final Remarks

At present, the scales required to fix Koide triplets are arbitrary, although the charged lepton scale happens to be 313.8 eV, very close to the dynamical quark scale [8]. However, the other Koide parameters are sufficiently constraining that we may begin to extend the low energy spectrum to standard higher mass states, observable at the LHC. The full Standard Model spectrum itself remains to be analysed.

This background independent approach does not require a traditional form of supersymmetry, since both classical manifolds and supermanifolds are viewed as emergent constructions. Moreover, a new kind of supersymmetry is recovered via a twisted Fourier transform that interchanges known fermions and bosons [16]. Thus there is no reason to expect superpartner observables, either at the LHC or in dark matter searches. There is no Higgs boson, since the Higgs mechanism is an effective local description that does not apply to real world quantum gravity. It's mathematical structure will be outlined in future work. There are no astrophysical quantum gravitational waves either, since gravity is non local.

Initial work on a non local version of the Standard Model [19][22][23][25] manifestly contains combinatorial elements of a categorical nature [19]. In particular, the on-shell BCFW recursion rules obey the structure of the associahedra polytopes for associator maps. In a categorical sense, these polytopes are all one dimensional. Twistor theorists have long sought a two or three dimensional analogue of this construction, since multiple twistor solutions to massless field equations may be combined to form higher dimensional cohomology classes, which represent rest mass. It is therefore expected that General Relativity will be recovered via a higher categorical form of the twistor framework, using octonion matrix theory.

The quantitative predictions resulting from neutral particle gravity are clearly falsifiable, but we are not as yet aware of any experimental data that conflicts with this point of view.

Acknowledgements

I am truly indebted to Michael Rios for numerous discussions on the physics, including cosmology, M theory, tree diagrams in twistor scattering theory, and the categorical context of all the above. Carl Brannen and Graham Dungworth have also contributed greatly to these ideas. Thank you also to the School of Chemical and Physical Sciences at the University of Victoria Wellington for its generous support.

[1] S. O. Bilson-Thompson, arXiv:hep-ph/0503213v2.

[2] G. Dungworth, http://www.galaxyzooforum.org/index.php?topic=277933.0.

[3] R. Penrose, in *Combinatorial Mathematics and its Applications* (Academic Press, 1971).

[4] R. Penrose, http://users.ox.ac.uk/ tweb/00001/.

[5] L. Riofrio, http://riofriospacetime.blogspot.com/2006/09/recent-gmtc3-paper.html.

[6] M. Pitkanen, http://matpitka.blogspot.com/.

[7] C. A. Brannen, Found. Phys. (2010), DOI: 10.1007/s10701-010-9465-8.

[8] C. A. Brannen (2008), http://www.brannenworks.com/koidehadrons.pdf.

[9] M. Rios, http://arxiv.org/abs/1005.3514.

[10] R. Penrose, http://accelconf.web.cern.ch/accelconf/e06/PAPERS/THESPA01.PDF.

[11] W. G. S. P. F. Harrison and D. H. Perkins, Phys. Lett. B **530**, 167 (2002), hep-ph/0202074.

[12] P. F. Harrison and W. G. Scott, Phys. Lett. B **547**, 219 (2002), hep-ph/0210197.

[13] M. D. Sheppeard, http://pseudomonad.blogspot.com/2010/06/minos-neutrinos-ii.html.

[14] B. Coecke and R. Duncan, in *ICALP (2)* (2008), pp. 298–310, http://arxiv.org/abs/0906.4725.

[15] M. D. Sheppeard, http://vixra.org/abs/1008.0015.

[16] M. D. Sheppeard, http://vixra.org/abs/1004.0083.

[17] I. M. Gelfand, M. M. Kapranov, and A. V. Zelevinsky, *Discriminants, Resultants and Multidimensional Determinants* (Birkhauser, 1994).

[18] M. D. Sheppeard, J. Math. Phys. **51**, 023507 (2010).

[19] M. D. Sheppeard, Ph.D. thesis, Canterbury (2007), http://hdl.handle.net/10092/1436.

[20] M. C. Shum, J. Pure Appl. Algebra **93**, 57 (1994), doi:10.1016/0022-4049(92)00039-T.

[21] S. Abramsky and B. Coecke, Proceedings of the 19th IEEE conference on Logic in Computer Science (LiCS'04) (2004), http://arxiv.org/abs/quant-ph/0402130.

[22] N. Arkani-Hamed, F. Cachazo, C. Cheung, and J. Kaplan (2009), arxiv: 0903.2110v2.

[23] N. Arkani-Hamed, F. Cachazo, C. Cheung, and J. Kaplan (2009), arxiv: 0907.5418v1.

[24] L. Mason and D. Skinner (2009), arxiv: 0903.2083.

[25] A. Hodges (2009), arxiv: 0905.1473.

[26] D. Bar-Natan, in *Proceedings of the Georgia international topology conference*, edited by W. H. Kazez, Amer. Math. Soc. (International Press, 1997), pp. 139–183, http://www.math.toronto.edu/drorbn/papers/nat/nat.pdf.

[27] H. Furusho, Annals of Math. **171**, 545–556 (2010).

[28] L. Borsten, D. Dahanayake, M. J. Duff, H. Ebrahim, and W. Rubens, Phys. Rev. A **80**, 032326 (2009), DOI:10.1103/PhysRevA.80.032326.

[29] MINOS Collaboration, http://www-numi.fnal.gov/PublicInfo/forscientists.html.

[30] R. Foot, Int. J. Mod. Phys. D **13**, 2161 (2004), arxiv:quant-ph/0402130.

[31] L. Riofrio, http://riofriospacetime.blogspot.com/.